

**Dispersity Control in Atom Transfer Radical Polymerizations
through Addition of Phenyl Hydrazine**

Journal:	<i>Polymer Chemistry</i>
Manuscript ID	PY-ART-01-2018-000033.R1
Article Type:	Paper
Date Submitted by the Author:	04-May-2018
Complete List of Authors:	Yadav, Vivek; University of Houston Hashmi, Nairah; University of Houston Ding, Wenyue; University of Houston Li, Tzu-Han; University of Houston Mahanthappa, Mahesh; University of Minnesota, Department of Chemical Engineering & Materials Science; University of Wisconsin-Madison, Department of Chemistry Conrad, Jacinta; University of Houston, Robertson, Megan; University of Houston, Chemical and Biomolecular Engineering

Dispersity Control in Atom Transfer Radical Polymerizations through Addition of Phenyl Hydrazine

Vivek Yadav,^a Nairah Hashmi,^a Wenyue Ding,^a Tzu-Han Li,^c Mahesh K. Mahanthappa,^d Jacinta C. Conrad,^{*a} and Megan L. Robertson^{*a,b}

^aDepartment of Chemical and Biomolecular Engineering
University of Houston, Houston, TX 77204-4004

^bDepartment of Chemistry
University of Houston, Houston, TX 77204-4004

^cMaterials Engineering Program
University of Houston, Houston, TX 77204-4004^dDepartment of Chemical Engineering and
Materials Science
University of Minnesota, Minneapolis, MN 55455

*E-mail: mlrobertson@uh.edu, jconrad@uh.edu

†Electronic Supplementary Information available online.

Abstract

Molar mass dispersity in polymers affects a wide range of important material properties, yet there are few synthetic methods that systematically generate unimodal distributions with specifically tailored dispersities. Here, we describe a general method for tuning the dispersity of polymers synthesized via atom transfer radical polymerization (ATRP). Addition of varying amounts of phenyl hydrazine (PH) to the ATRP of *tert*-butyl acrylate led to significant deviations in the reaction kinetics, yielding poly(*tert*-butyl acrylate) with dispersities $\bar{D} = 1.08 - 1.80$. ATRP reactions in the presence of the reducing agent tin (II) 2-ethylhexanoate, under otherwise comparable reaction conditions, did not drive similar increases in dispersity. We therefore deduced that PH does not function primarily as a reducing agent in these syntheses. Nuclear magnetic resonance analyses revealed the incorporation of aromatic polymer end-groups upon PH addition, suggesting that the ATRP-active halide termini of the growing polymer chains underwent irreversible nucleophilic substitution reactions with PH that led to chain termination. A kinetic model including this irreversible chain termination by PH was in excellent agreement with experimentally measured reaction kinetics. To demonstrate the generality of this approach, we conducted ATRP syntheses of polystyrene in the presence of PH to achieve dispersities of $\bar{D} = 1.07 - 2.30$. This study suggests that PH addition is an effective, facile, and flexible method of dispersity control in polymers synthesized by ATRP.

Introduction

Molar mass dispersity (\bar{D}), defined as the ratio of weight-average and number-average molecular weights, provides a quantitative measure of the breadth of the molecular weight distribution of a polymer. This distribution crucially governs diverse polymer physical properties. For example, increasing \bar{D} can improve the processability of polymer melts by delaying the onset of flow instabilities.¹⁻³ Dispersity greatly impacts the rheological properties of polymers, including the steady shear, zero shear, and elongational viscosities, storage and loss moduli, and normal stresses.⁴⁻⁹ Additionally, dispersity plays an important role in polymer phase behavior, enabling tunable blend miscibility¹⁰⁻¹² and block copolymer morphologies and domain spacings.¹³⁻¹⁹ Dispersity also alters the mechanical behavior of polymers, such as the modulus of a block copolymer.²⁰ In polymer brushes, increased \bar{D} can further induce conformational changes,²¹ which alter the pH-responsive behavior of polyelectrolyte brushes^{22, 23} and impart greater stability to polymer-grafted nanoparticles.²⁴

Various approaches have been developed to tune the dispersity in different classes of polymers. Blending polymers of differing molecular weights, which gives rise to multimodal molecular weight distributions, is an often employed yet inefficient method to increase dispersity.^{4-6, 25, 26} Through choice of catalyst and reaction temperature or exogenous addition of various chain transfer agents, the molecular weight distributions of polymers synthesized by Ziegler-Natta and metallocene polymerizations can be modified to yield polymers with $\bar{D} = 1.1 - 42$, typically with bimodal distributions when the dispersity is high ($\bar{D} \geq 2$).^{3, 27-30} By controlling the monomer conversion and rate of transesterification in ring-opening transesterification polymerization (ROTEP) of cyclic esters, the dispersities of the resulting polyesters can be tuned over the range of $\bar{D} = 1.1 - 2.0$.¹³ Similarly, the dispersities of polymers produced through anionic polymerization can be systematically increased over a limited range ($\bar{D} \leq 1.34$) by carefully-metered addition of a *sec*-butyllithium initiator or by increasing the reaction temperature.^{9, 14} The limited monomer scope associated with each of these polymerization processes, however, curtails the broad applicability of each method of dispersity control. Hence, an open challenge is to develop a more widely applicable method of synthesizing polymers with unimodal molecular weight distributions and tunable dispersities, thereby enabling the development of new polymeric materials with unusual properties.

Radical polymerization methodologies provide convenient access to a diverse range of polymers. For the free radical polymerizations commonly used in commercial polymer production, the “most probable” molecular weight distribution originally anticipated by Carothers³¹ exhibits $\bar{D} = 1.5 - 2$ (depending on the relative rates of chain termination by radical recombination and disproportionation). Branching, chain coupling, or other unintended side reactions may lead to multimodal distributions with $\bar{D} > 2$. Controlled radical polymerizations,

by contrast, provide access to low dispersity polymers ($D < 1.1$) with unimodal distributions.³²⁻³⁴ A recent study employing nitroxide-mediated polymerization (NMP), a variant of controlled radical polymerization, described an approach to vary dispersity through the metered addition of initiator, modifying not only the breadth but also the shape of the molecular weight distribution.³⁵ Though of great utility in solution polymerizations, an approach using metered initiator addition cannot be applied to polymerizations in the absence of a solution initiator, such as in surface-initiated polymerizations. Furthermore, NMP suffers from limitations of slow polymerization kinetics, lack of applicability to methacrylate monomers, and challenging reagent syntheses (e.g. nitroxides).³⁶ Methods for dispersity control have also been developed for reversible addition-fragmentation chain-transfer (RAFT) polymerizations, which are more widely applicable to diverse monomer types than NMP. Boyer and collaborators have investigated photoinduced electron/energy transfer RAFT polymerization in combination with a flow process, to produce solution polymers of varying molecular weight distributions (through the collection of fractions of differing molecular weight produced throughout the total reaction time).³⁷ However, this method also cannot be applied to surface-initiated polymerizations. An alternative approach is to use atom transfer radical polymerization (ATRP), another variant of controlled polymerization.³⁸ ATRP is applicable to diverse monomers and is widely used in both solution and surface-initiated polymerizations.³⁹ Thus, it is of much interest to develop methods to tune dispersity in both solution and surface-initiated ATRP syntheses.

Copper-catalyzed ATRP reactions typically employ metal complexes of the type $LCu^I X$, where L is a multidentate nitrogen-based ligand and $X = Cl$ or Br . These metal complexes reversibly react with activated alkyl halide initiators through single-electron, inner sphere atom transfer oxidation reactions to yield $LCu^{II} X_2$ and alkyl free radicals. If the rates of Cu-catalyzed

alkyl free radical formation and deactivation are much faster than the rate of radical chain propagation, uniform chain growth occurs to give rise to narrow dispersity polymers.³² Thus, suitable choices of polymerization initiator and $\text{LCu}^{\text{I}}\text{X}$ catalyst for a given monomer lead the propagating chain ends to spend a majority of their time in their deactivated (or dormant) states, thereby limiting the chain termination side reactions. Although low dispersity ($D < 1.1$) polymers may be readily synthesized with ATRP techniques, there remains an unmet need for ATRP processes that produce polymers with unimodal molecular weight distributions and tunable dispersities.

Because ATRP is a variant of free radical polymerization, poor choices of Cu catalyst and initiator for given monomer can enable chain termination reactions that yield polymers with high dispersities. For example, many studies document the synthesis of polyacrylates, polymethacrylates, and polystyrenes with $D = 1.1 - 3.0$ by varying the ATRP reaction temperature, pressure, catalyst/ligand, initiator, and/or solvent.^{32, 40-46} As these approaches to varying dispersity arise from poorly controlled polymerizations, they do not provide a rational and reliable method to controllably and systematically vary polymer dispersity. In related syntheses of poly(*n*-butyl acrylate) by Activators Regenerated by Electron Transfer (ARGET) ATRP that employ low concentrations of the Cu catalyst (< 50 ppm),³⁸ the addition of reducing agents such as phenylhydrazine and hydrazine led to $D = 1.23 - 2.3$.⁴⁷ These variations in dispersity again arose as an unintended consequence of optimizing the ARGET ATRP method, and the mechanism by which the dispersity increases in the presence of phenylhydrazine and hydrazine remains obscure.

Herein, we develop a method for systematically varying the dispersity of polymers produced by ATRP through the exogenous addition of phenylhydrazine (PH). Using

conventional ATRP conditions with stoichiometrically balanced amounts of Cu-catalyst and an activated alkyl halide initiator, we demonstrate that PH addition enables the synthesis of poly(*tert*-butyl acrylate) (PtBA) with $\bar{D} = 1.08 - 1.80$. PH addition to Cu-mediated ATRP reactions modified the reaction kinetics and broadened the molecular weight distributions. To determine whether the mechanism of action of PH in these polymerizations stemmed from its ability to act as a reducing agent for oxidized catalyst species, we added the reducing agent tin(II) 2-ethylhexanoate to ATRP reactions conducted under otherwise identical conditions. These comparative studies revealed that PH does not act as a reducing agent. Instead, as confirmed through NMR analysis of the polymer end-groups, PH irreversibly reacts with the polymeric alkyl halide by nucleophilic substitution, terminating the chains. The reaction kinetics in the presence of PH are described by a simple kinetic model. We apply these mechanistic insights to rationally synthesize polystyrenes with $\bar{D} = 1.07-2.30$, thus showcasing the generality of this synthetic methodology in enabling molar mass dispersity control in ATRP reactions.

Materials and Methods

Materials. All chemicals were purchased from Sigma-Aldrich (Milwaukee, WI) and used as received unless otherwise noted. Monomethyl ether hydroquinone (inhibitor) was removed from *tert*-butyl acrylate (tBA, 98%) by passage through a silica gel column (60 Å pore size). tBA was then dried over calcium hydride (reagent grade, 95%) and distilled under vacuum. Ethyl α -bromoisobutyrate (EBiB, 98%) and *N,N,N',N',N''*-pentamethyldiethylenetriamine (PMDETA, 99%) were each degassed with three freeze-pump-thaw cycles. 4-*tert*-butylcatechol was removed from styrene (99%) by passage through a basic alumina column (58 Å pore size). Toluene (JT Baker, HPLC grade, 99.7%) was dried using a Pure Process Technology solvent purification system.

Characterization. Gel permeation chromatography (GPC) was employed to characterize the number-average molecular weight (M_n), weight-average molecular weight (M_w), and dispersity (D) of each polymer. The polymers were analyzed with a Viscotek GPC system equipped with two Agilent ResiPore columns and refractive index, right- and low-angle light scattering, and viscometer detector modules. Samples were analyzed using stabilized THF (OmniSolv, HPLC grade, >99.9%) as the mobile phase at 30°C with flow rate of 1 mL min⁻¹, injection volume of 100 μL, and sample concentration of 1 mg mL⁻¹. Linear polystyrene (PS) standards were used for calibration (9 Viscotek PolyCAL Standards obtained from Malvern, with molecular weight at the peak maximum, M_p , of 1.05, 2.79, 6.04, 13.4, 29.6, 64.5, 98.1, 170, and 400 kg mol⁻¹, reported by the supplier). Triple detection with light scattering was used where applicable; the low refractive index increment of poly(*tert*-butyl acrylate) in THF, however, precluded light scattering analysis of low molecular weight polymers.

Proton nuclear magnetic resonance (¹H NMR) spectra were collected on a JEOL ECA-500 spectrometer using deuterated chloroform as the solvent. Chemical shifts were referenced to the residual protiated solvent resonance (δ 7.26 ppm).

Representative ATRP Synthesis of Poly(*tert*-butyl acrylate) (PtBA). PtBA was synthesized using atom transfer radical polymerization (ATRP).^{23, 48-50} In a nitrogen glovebox, equimolar amounts of PMDETA (24.3 μL), copper(I) bromide (CuBr, 99%, 16.7 mg), and EBiB (initiator, 16.8 μL) were combined in a 50-mL round bottom flask containing a 1:1.75 v:v solution of tBA (2 mL) in anhydrous N,N-dimethylformamide (DMF, 99.8%, 3.5 mL), with [tBA]:[EBiB]:[CuBr]:[PMDETA] = 120:1:1:1. The final concentration of CuBr was 0.021 M. The flask was capped with a septum inside of the glove box and transferred to a preheated oil bath at 50°C. Following the desired reaction time, the polymerization was quenched by addition

of around 5 mL tetrahydrofuran (THF, OmniSolv, HPLC grade, 99.9%) and exposure of the reaction mixture to air. The reaction solution was further diluted with excess THF and passed through a neutral aluminum oxide column to remove the catalyst. The catalyst-free polymer solution was concentrated using a rotary evaporator and precipitated in a DI water/methanol mixture (1:1 v:v). Finally, the precipitated PtBA was collected and dried under vacuum overnight at ambient temperature. To obtain polymers with variable dispersities, PH (97%) was added to the reaction mixture. With all other stoichiometries and conditions as described above, the ratio [PH]:[EBiB] was varied (0:1, 1:1 and 3:1). In select reactions, tin(II) 2-ethylhexanoate (95%) was added in place of PH. To monitor reaction kinetics, aliquots were taken from the reaction mixture at different reaction times and quenched with THF in the presence of air prior to purification.

Representative ATRP Synthesis of Polystyrene (PS). PS was also synthesized using ATRP. Equimolar amounts of PMDETA (24.3 μL) and EBiB (16.8 μL) were combined in a 50-mL round bottom flask containing a 1:1.75 v:v solution of styrene (1.57 mL) in anhydrous toluene (2.75 mL), with [styrene]:[EBiB]:[PMDETA] = 120:1:1, and purged with argon for 30 min. A second 50-mL round bottom flask was prepared containing CuBr (16.7 mg) and purged with argon for 30 min. An equimolar amount of CuBr (in second flask) and PMDETA (in first flask) was used. After purging, the contents from the first flask were transferred to the second flask using a cannula tube. The final concentration of CuBr was 0.027 M. The reaction mixture was heated in a preheated oil bath at 80°C. Following the desired reaction time, the polymerization was quenched by addition of around 5 mL THF and exposure of the reaction mixture to air. The reaction solution was further diluted with excess THF and was passed through a neutral aluminum oxide column to remove the catalyst. The catalyst-free polymer

solution was concentrated using a rotary evaporator and precipitated in methanol. Finally, the precipitated PS was collected and dried under vacuum overnight at ambient temperature. To obtain polymers with variable dispersities, PH (97%) was added to the reaction mixture. With all other stoichiometries and conditions as described above, the ratio [PH]:[EBiB] was varied (0:1, 0.2:1, 1:1, and 3:1). To monitor reaction kinetics, multiple reactions were conducted under analogous stoichiometries and conditions, and quenched at different reaction times.

Results and Discussion

Reaction Kinetics and Polymer Characteristics Observed in the ATRP of tert-Butyl Acrylate

To explore the impact of added phenyl hydrazine (PH) on the Cu-catalyzed ATRP of *tert*-butyl acrylate (tBA), we first developed a standard set of polymerization reaction conditions and methods. Based on prior studies,⁴⁸⁻⁵⁰ we employed an EBiB-initiated reaction with catalyst CuBr/PMEDA in a 50 vol% solution of tBA in DMF. Aliquots of the reaction mixture were periodically removed and subjected to quantitative ¹H NMR spectroscopy to assess the tBA conversion, by integrating the spectral resonances associated with the *tert*-butyl group of the unreacted monomer (δ 1.47 ppm) and the monomers within the polymer (δ 1.41 ppm) (Figures S1 – S2 in the ESI). Additionally, we calculated the theoretical $M_{n,th} = (\text{conversion}) \cdot [M]_0 / [I]_0$ where $[M]_0$ and $[I]_0$ are the initial monomer and initiator concentrations, respectively. From these reaction aliquots, we isolated purified polymer samples. To quantify $M_{n,GPC}$, the purified polymers were characterized with GPC against polystyrene standards (Figure S3 in the ESI). To calculate $M_{n,NMR}$, purified polymers were characterized via quantitative ¹H NMR end-group analysis, using the areas of the peaks associated with the isobutyrate methyl groups (-C(O)-CMe₂-) of the initiator fragment and the *tert*-butyl group (-O-CMe₃) of PtBA repeat units (see ESI for additional details).⁵¹⁻⁵⁵

The resulting reaction kinetics data, M_n as a function of conversion, are shown for the ATRP of tBA without PH addition in Figure 1a (detailed data are provided in Table S1 in the ESI). GPC traces of aliquots acquired at different reaction times indicate the formation of polymers with unimodal and narrow molecular weight distributions ($D \leq 1.11$) across all conversions (Figure 1b). Quantitative kinetics analyses reveal that $M_{n,th}$ determined from the

monomer conversion agreed remarkably well with the experimentally determined $M_{n,GPC}$ and $M_{n,NMR}$ values, all of which linearly increased with conversion as expected for a well-controlled ATRP reaction. We note that modest deviations in the values of $M_{n,NMR}$ and $M_{n,GPC}$ are expected, given the latter values were determined against narrow dispersity polystyrene standards. Due to a dramatic increase in reaction viscosity and observed deviations in the linearity of M_n vs. conversion at these high monomer conversions, we studied the kinetics of this control reaction only up to 85% monomer conversion (180 min reaction time).

Impact of Phenyl Hydrazine on the ATRP of tert-Butyl Acrylate

Using the ATRP of tBA as a model reaction and the analysis methods described above, we examined the effect of two different concentrations of PH ([PH]:[EBiB] = 1:1 and 3:1) under otherwise identical reaction conditions. In the presence of PH, the monomer conversion and M_n plateaued after a given reaction time (Table S1 in the ESI). The maximum achievable monomer conversion decreased substantially upon increasing the PH concentration in the reaction (Table 1). Furthermore, the addition of increasing amounts of PH induced a monotonic decrease in the $M_{n,GPC}$ for the isolated polymers at maximum monomer conversion. Notably, the dispersities of the isolated polymers were significantly higher than that obtained in the control polymerization without PH (Table 1).

Table 1. Characteristics of PtBA synthesized through ATRP with PH addition^a

[PH]:[EBiB]	t (min)	Conversion ^b	M_n (kg mol ⁻¹) ^c	D^c
0:1	180	85%	12.0	1.08
1:1	180	68%	9.6	1.80
3:1 ^d	120	36%	4.8	1.71

^a [tBA]:[EBiB]:[CuBr]:[PMDETA] = 120:1:1:1, 50 °C, DMF

^b Characterized through ¹H NMR (Figures S1 – S2, S4 – S5, S7 – S8 in the ESI)

^c Characterized through GPC (polystyrene standards, Figures S3, S6, S9 in the ESI)

^d Data are shown at 120 min for [PH]:[EBiB] = 3:1 as the conversion exhibited a plateau at shorter reaction time (Table S1 in the ESI)

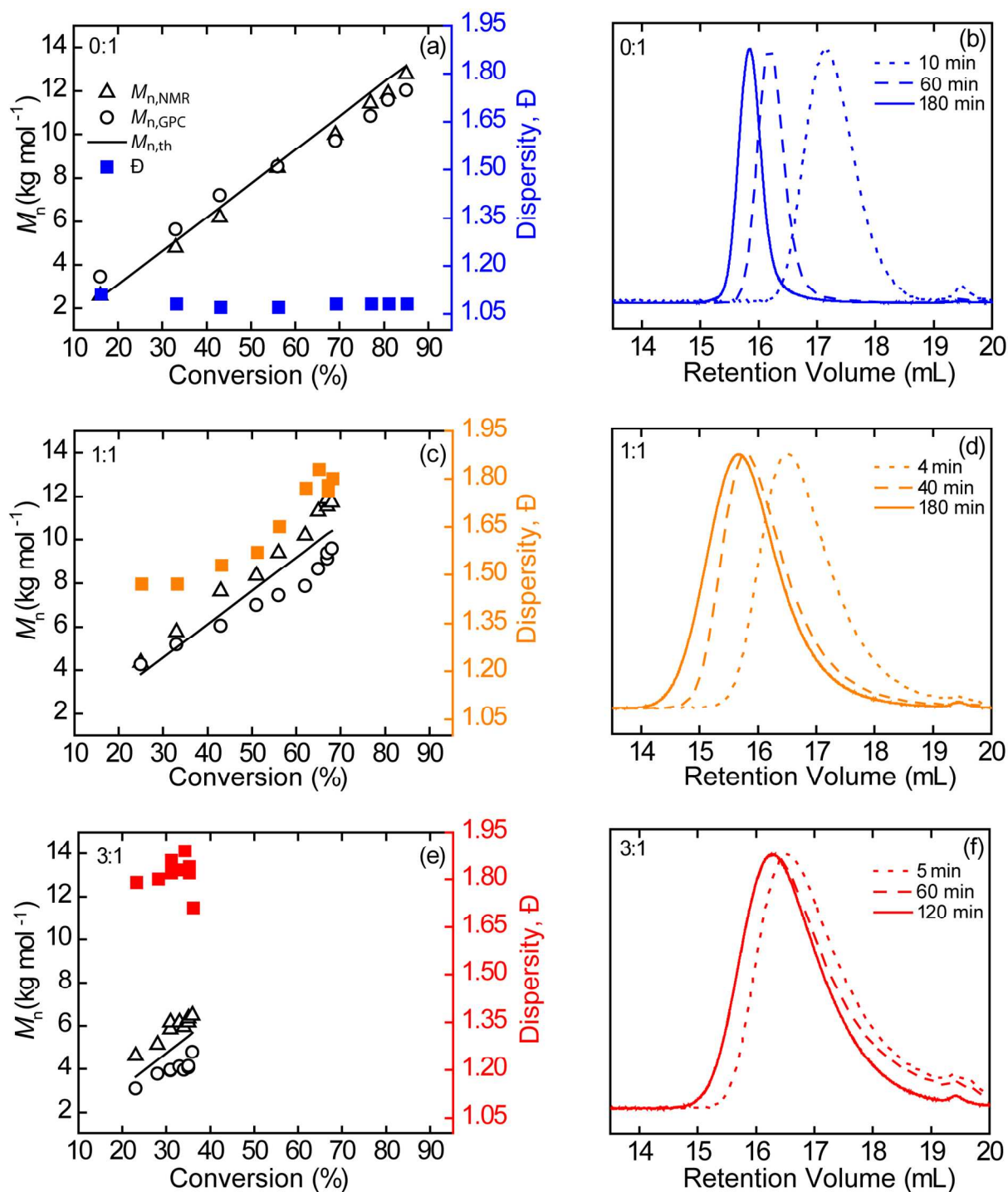


Figure 1. (a, c, e) M_n (left y-axis, open symbols) and dispersity D (right y-axis, closed symbols) as functions of monomer conversion for the ATRP of tBA containing different ratios of [PH]:[EBiB] (0:1, 1:1 and 3:1). (b, d, f) Representative GPC traces at different reaction times for

different ratios of [PH]:[EBiB]. Symbols denote the M_n characterized by NMR end-group analysis ($M_{n,NMR}$, Δ) and GPC ($M_{n,GPC}$, polystyrene standards, \circ), and the theoretical M_n from NMR conversion ($M_{n,th}$, solid line), as well as the dispersity \mathcal{D} calculated by GPC (polystyrene standards, \blacksquare). Increasing [PH]:[EBiB] leads to an increase in dispersity of the polymer. The small peak around 19.5 mL in the GPC traces originates from the solvent. The following reaction conditions were used: [EBiB]:[CuBr]:[PMDETA]:[tBA] = 1:1:1:120, 50 °C, DMF.

The addition of PH altered both the reaction kinetics and the molecular weight distribution of the polymer. Adding PH at a ratio of [PH]:[EBiB] = 1:1 produced a plateau in the monomer conversion at moderate reaction times, decreasing the maximum achievable conversion to 68%, and increased the molar mass dispersity \mathcal{D} (Figure 1(c)). In the presence of PH, \mathcal{D} also increased with conversion (from 1.47 at 25% conversion to 1.80 at 68% conversion). The width of the peak in the GPC data was greater than that observed in the absence of PH addition and increased with reaction time (Figure 1(d)). When the concentration of PH was increased further to [PH]:[EBiB] = 3:1, the maximum achievable conversion was reduced to 36% (Figure 1(e)). A small increase in conversion, from 23% to 36%, was observed over 120 minutes, and \mathcal{D} was close to 1.80 for all conversions, with the peak width in the GPC data exhibiting little change with reaction time, indicating loss of polymerization under this condition (Figure 1(f)). Complete ^1H NMR and GPC data obtained from reaction aliquots for all three PH loadings ([PH]:[EBiB] = 0:1, 1:1, and 3:1) are provided in Figures S1 – S9 and Table S1 in the ESI.

The data presented in Figure 1 reveal several distinctive features of polymers synthesized in the presence of PH. Adding PH reduced the maximum attainable conversion and broadened the molecular weight distribution. Whereas $M_{n,th}$, $M_{n,NMR}$, and $M_{n,GPC}$ were consistent for the PH-free polymerizations (Figure 1(a)), addition of PH led to a noticeable increase in $M_{n,NMR}$ as compared to $M_{n,th}$ and $M_{n,GPC}$ (Figures 1(c) and 1(e)). Further, reactions with added PH initially progressed more quickly than those without PH, as conversion around 25% was reached for both

1:1 and 3:1 samples within 5 minutes (Table S1 in the ESI). The mechanistic origins of this behavior will be discussed in more detail below.

The addition of PH to ATRP syntheses provides a flexible route to tuning dispersity, while still controlling M_n . The series of polymers shown in Figure 2 have similar M_n (around 6 kg mol⁻¹) yet \mathcal{D} varying from 1.07 – 1.71. Whereas M_n is readily varied through changing the monomer to initiator ratio or reaction time, \mathcal{D} is tuned through changing the concentration of PH relative to initiator (EBiB). Thus, it is possible to identify appropriate reaction conditions to produce a polymer of desired M_n and \mathcal{D} . We note that in addition to the solution syntheses presented in this manuscript, our group has previously demonstrated that the addition of PH can be used to tune dispersity in the surface-initiated ATRP of PtBA.^{22, 23}

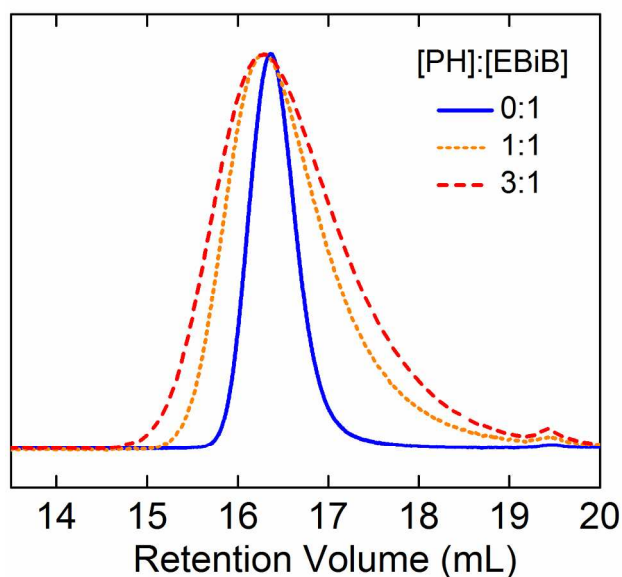


Figure 2. Variation in molecular weight distribution (shown as GPC traces) with phenyl hydrazine content for three polymers of similar M_n . The following reaction conditions were used: [EBiB]:[CuBr]:[PMDETA]:[tBA] = 1:1:1:120, 50 °C, DMF. [PH]:[EBiB] = 0:0 (blue solid curve, $\mathcal{D} = 1.07$, $M_{n,NMR} = 6.2$ kg mol⁻¹, 40 min reaction time); 1:1 (orange dotted curve, $\mathcal{D} = 1.47$, $M_{n,NMR} = 5.8$ kg mol⁻¹, 8 min reaction time); 3:1 (red dashed curve, $\mathcal{D} = 1.71$, $M_{n,NMR} = 6.5$ kg mol⁻¹, 120 min reaction time).

Models to Describe ATRP Reaction Kinetics

We compared the kinetics of the polymerizations conducted in the presence and absence of PH with two widely-accepted formalisms that describe well-controlled ATRP reactions (Scheme 1 illustrates ATRP equilibrium and propagation reactions). Fischer and co-workers noted that ATRP reactions conducted with highly purified Cu(I) salts exhibit a “persistent radical effect,” whereby the initial concentration of Cu(II) species is so low that radical termination dominates at short reaction times.⁵⁶ These radical termination events lead to the accumulation of Cu(II) species, which subsequently serve to control the ATRP reaction. Under those conditions, the reaction kinetics conform to the expression^{56, 57}

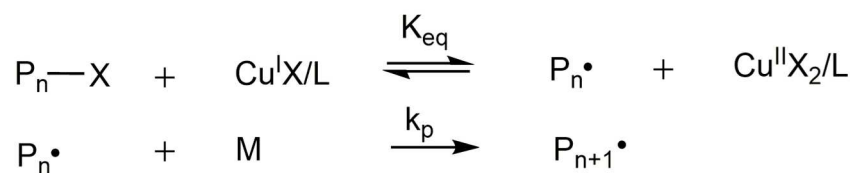
$$\ln \left(\frac{[M]_0}{[M]} \right) = \frac{3}{2} k_p ([RX]_0 [Cu(I)]_0)^{1/3} \left(\frac{K_{eq}}{3k_t} \right)^{1/3} t^{2/3} = K_{Fischer} t^{2/3} \quad (1)$$

where k_p and k_t are the respective rate constants for chain propagation and chain termination, K_{eq} is the equilibrium constant for the ATRP single-electron, inner sphere atom transfer reaction, $[M]$ and $[M]_0$ are the time-dependent and initial monomer concentrations, and $[RX]_0$ and $[Cu(I)]_0$ are the initial concentrations of the alkyl halide initiator (X typically is Br or Cl) and the Cu(I) catalyst species. Conversely, Matyjaszewski and coworkers noted that if the Cu salts used in forming the ATRP catalyst are impure due to adventitious oxidation of Cu(I) to Cu(II), self-regulation of the polymerization by the persistent radical effect becomes less important.⁵⁸ Under those conditions, Matyjaszewski and co-workers demonstrated that the reaction kinetics obey the rate expression⁵⁸

$$\ln \left(\frac{[M]_0}{[M]} \right) = k_p K_{eq} \frac{[RX]_0 [Cu(I)]_0}{[Cu(II)]_0} t = K_{App} t \quad (2)$$

where $[Cu(II)]$ refers to the concentration of Cu(II) species present in the reaction. Experimental work on methyl methacrylate demonstrated that eqn 1 applies when $[Cu(II)]_0/[Cu(I)]_0 < 0.1$, whereas eqn 2 applies when $[Cu(II)]_0/[Cu(I)]_0 > 0.1$ with a crossover at $[Cu(II)]_0/[Cu(I)]_0 =$

0.1.⁵⁷ The exact crossover ratio, however, depends on the rate constants and varies from one reaction system to another.⁵⁹



Scheme 1. ATRP equilibrium and propagation reactions.

The kinetics of the reaction without PH were in excellent agreement with the prediction of both eqns 1 and 2 (Figure 3), suggesting that the ratio of $[Cu(II)]_0/[Cu(I)]_0$ in our system is close to the crossover value. We observed, however, that addition of PH to the ATRP of tBA led to a five-fold decrease in the time required to achieve ~25% monomer conversion, suggesting a faster rate of initial monomer consumption induced by PH (Table S1 in the ESI). Indeed, the rate of initial monomer consumption at short reaction times (c.f. Figure 3) is faster than anticipated by either eqn 1 or 2. The maximum achievable conversion decreases upon addition of increasing amounts of PH, accompanied by the appearance of a plateau in the monomer conversion at shorter reaction time. Previous studies have attributed plateaus in monomer conversion to irreversible chain termination reaction,^{60,61} suggesting this possibility in these polymerizations.

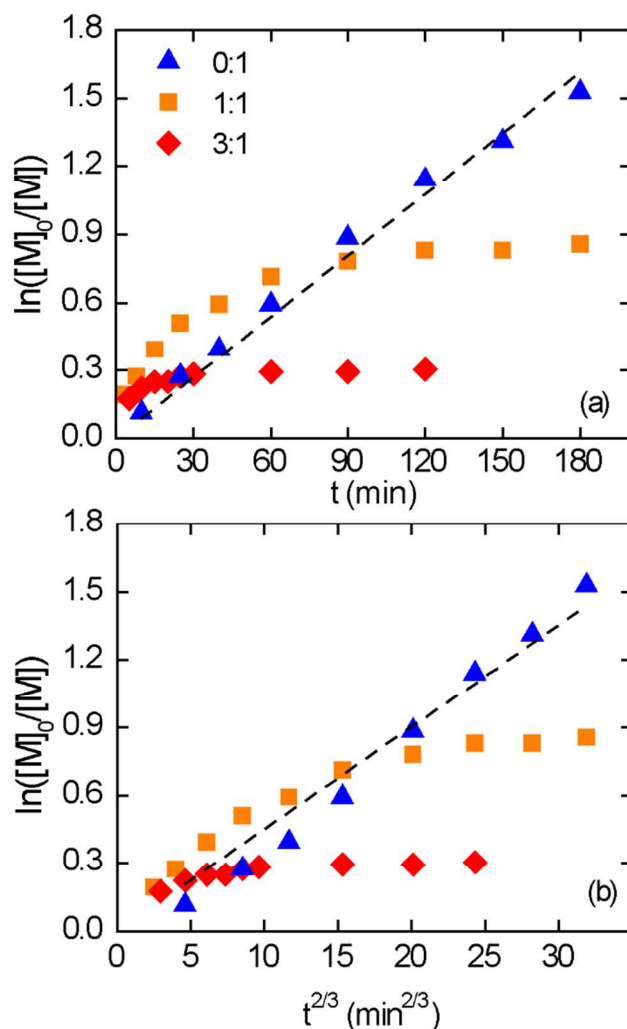


Figure 3. $\ln([M]_0/[M])$ as a function of reaction time (a) t and (b) $t^{2/3}$, corresponding to Matyjaszewski's (a) and Fisher's (b) ATRP kinetics schemes, respectively, for the ATRP of tBA containing different ratios of $[PH]:[EBiB]$: 0:1 (blue \blacktriangle), 1:1 (orange \blacksquare), and 3:1 (red \blacklozenge). Increasing $[PH]:[EBiB]$ leads to lower final conversion and significant deviations from both kinetics schemes. For the polymerization in the absence of PH (0:1), both Matyjaszewski's and Fisher's equations provided a good fit ($R^2 = 0.99$ for Matyjaszewski's equation and $R^2 = 0.98$ for Fisher's equation).

Mechanism of Increased Dispersity in ATRP Syntheses Conducted with PH

Two mechanisms may underlie the observed increase in polymer dispersity with the addition of PH: 1) addition of a reducing agent leads to deviation from ATRP kinetics, and/or 2) the presence of side reactions with PH leads to irreversible chain termination. To test the first

mechanism, we conducted ATRP reactions in which we substituted the reducing agent tin(II) 2-ethylhexanoate ($\text{Sn}(\text{oct})_2$)^{62, 63} in place of PH under otherwise identical conditions (NMR data provided in Figure S10 in the ESI). GPC analyses indicated that neither increasing the reaction time nor the concentration of $\text{Sn}(\text{oct})_2$ with respect to initiator significantly increased the dispersities of the isolated polymers, which were $\text{Đ} \sim 1.1$ in all cases (Table 2 and Figure 4(a)). Likewise, GPC analyses showed little change in the breadth of the molecular weight distribution upon addition of $\text{Sn}(\text{oct})_2$ when compared to that obtained without addition of a reducing agent (Figure 4(b)). Only when PH was added did the breadth of the molecular weight distribution markedly increase (Figure 4(b)). These results indicate that the ability of PH to increase dispersity is not due to its generic action as a reducing agent, but is instead specific to this compound.

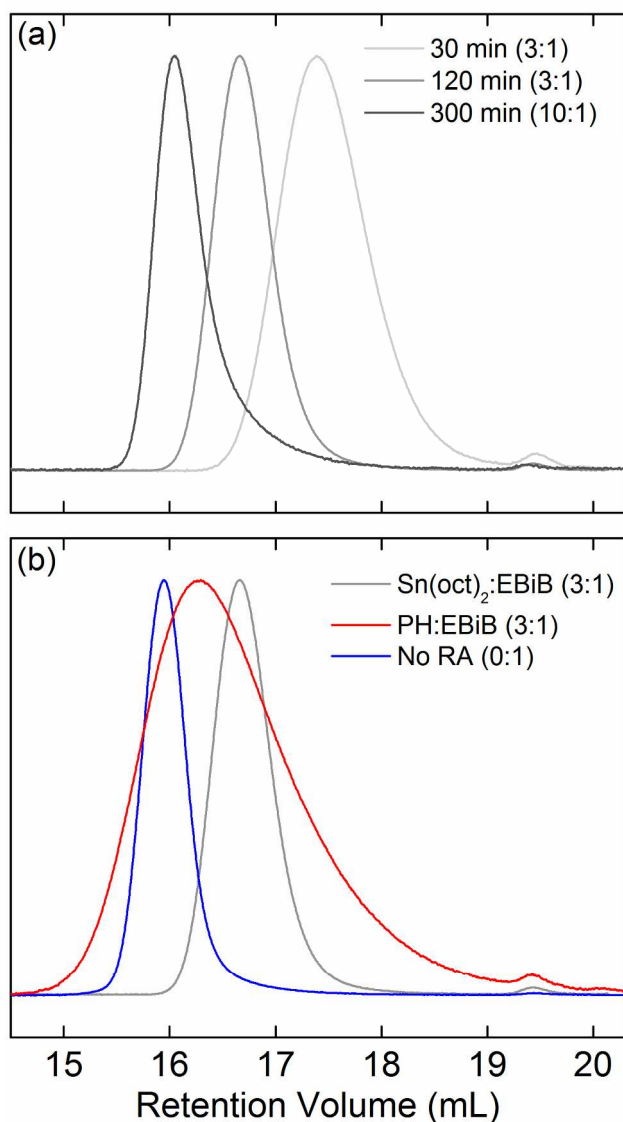


Figure 4. (a) GPC traces of polymers obtained from the ATRP of tBA in the presence of various ratios of Sn(oct)₂ to EBiB (3:1 and 10:1) and at different reaction times (30, 120, and 300 min). (b) Comparison of GPC traces of polymers obtained in the presence of Sn(oct)₂ or PH, and in absence of any reducing agent (RA), after a reaction time of 120 min. Adding Sn(oct)₂ does not significantly change the breadth of the molecular weight distribution in comparison to the reaction with no reducing agent, whereas adding PH greatly broadens the molecular weight distribution. The small peak around 19.5 mL in the GPC traces is from the solvent.

Table 2. Characteristics of PtBA synthesized through ATRP with addition of Sn(oct)₂^a

[Sn(oct) ₂]:[EBiB]	Time (min)	Conversion ^b	M_n (kg mol ⁻¹) ^c	\mathcal{D} ^c
3:1	30	18%	2.9	1.11
3:1	120	39%	5.5	1.07
10:1	300	47%	8.6	1.12

^a [tBA]:[EBiB]:[CuBr]:[PMDETA] = 120:1:1:1, 50 °C, DMF

^b Characterized through ¹H NMR (Figure S10 in the ESI)

^c Characterized through GPC (polystyrene standards, Figure 4a))

The lack of increase in \mathcal{D} for ATRP reactions of tBA conducted with Sn(oct)₂, coupled with the observed changes in the presence of PH (faster rate of monomer conversion, decrease in maximum monomer conversion, and increase in \mathcal{D}) suggest that PH induces irreversible chain termination. The consistent and significant positive deviation of $M_{n,NMR}$ as compared to $M_{n,th}$ suggests a possible loss of activated bromide end-group fidelity, which could lead to erroneously high values of $M_{n,NMR}$. Thus, we hypothesize that premature chain termination in PH-loaded polymerizations may occur by some interaction or reaction of PH with the activated bromide end-groups of the ATRP-active polymer chains.

NMR spectra obtained from PtBA synthesized in the presence of PH revealed aromatic resonances in the range δ 7.08 – 7.24 ppm (Figure 5(a) and Figures S4 and S7 in the ESI), which do not appear for polymers produced in the absence of PH (Figure S1 in the ESI). The activated bromide species 1-phenylethyl bromide (a low molecular weight analogue of bromine-terminated polystyrene chains) is known to react with nucleophiles such as PH and hydrazine via nucleophilic substitution.⁶⁴ Thus, it is possible that PH reacts directly and irreversibly with the activated bromide chain end during the course of the polymerization, which was conducted in a polar aprotic solvent (DMF) that favors this type of S_N2 reaction. Such a reaction would then

terminate the growing chains and lead to a loss of control in the ATRP reaction, consistent with the higher dispersities and lower maximum monomer conversions observed in the presence of PH.

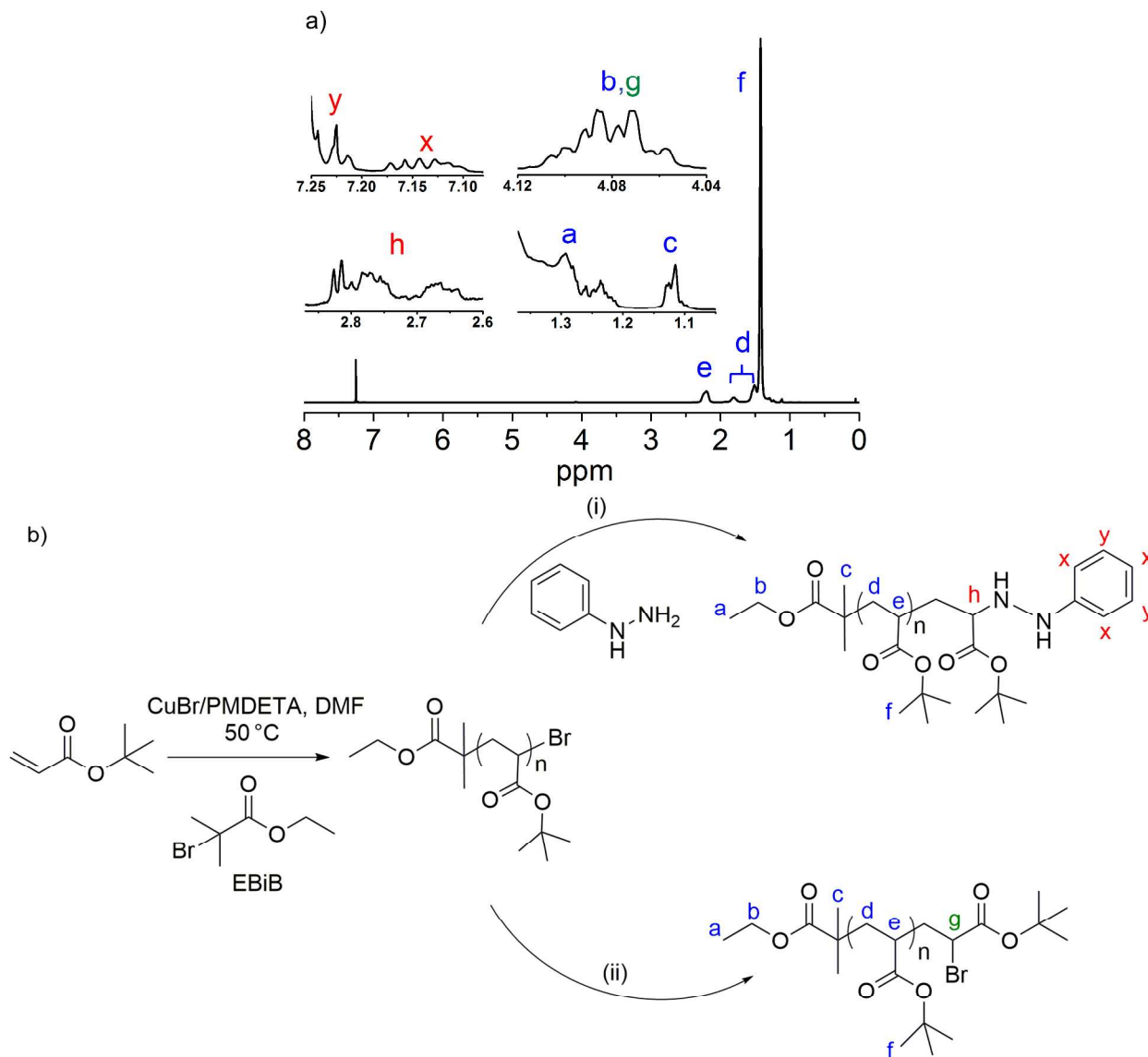


Figure 5. (a) ^1H NMR data obtained from PtBA polymerized through ATRP with PH addition ($[\text{PH}]:[\text{EBiB}] = 1:1$). The following reaction conditions were used: $[\text{EBiB}]:[\text{CuBr}]:[\text{PMDETA}]:[\text{tBA}] = 1:1:1:120$, $50\text{ }^\circ\text{C}$, DMF. Additional NMR spectra are shown in Figures S1 – S2, S4 – S5, and S7 – S8. Peaks x, y, and h are absent when PH is not added to the reaction. (b) Reaction mechanism for ATRP synthesis of PtBA conducted in the (i) presence and (ii) absence of PH. NMR peak positions corresponding to labeled protons are indicated in Figure 5(a). Addition of PH leads to chain termination reactions with alkyl halides, producing aromatic end groups (labeled x, y, and h) and reducing the concentration of Br-containing end groups (labeled g), as quantified in Table 3.

In search of evidence for irreversible chain termination of the activated bromide end-groups of PtBA by nucleophilic substitution with PH, we quantified the end-group fidelities of

our isolated polymers as a function of PH addition (a representative NMR spectrum is shown in Figure 5(a), with peak labels referenced to the chemical structure of the polymer shown in Figure 5(b)). Specifically, we compared the peak areas corresponding to the methyl groups of the initiator fragment on the polymer chain end (peak c) to the overlapping peak areas of the methylene group of the initiator fragment on the polymer chain end (peak b) and the CH on the Br end-group (peak g). The peak area ratio c:(b+g) was close to the theoretical value of 2 in the absence of PH, but markedly increased with addition of PH (Table 3).

Using the peak areas of the end-groups, we calculated the extent of the side reaction (Table 3), defined as $100 \cdot (2A_x)/(A_c)$, where A_x and A_c are the respective areas of peaks x and c. The yield of substituted alkyl chains increased from 38% to 53% upon increasing [PH]:[EBiB] from 1:1 to 3:1. This result confirms that addition of PH leads to nucleophilic substitution reactions, with the extent of the substitution reaction increasing with PH concentration. We further confirmed the presence of PH-terminated chains through Matrix-Assisted Laser Desorption/Ionization–Time of Flight (MALDI-TOF) Spectroscopy, described in the Electronic Supplementary Information (Figures S11-S14 and Table S3). The proposed reaction mechanism by which addition of PH increases the polymer dispersity via chain termination is shown in Figure 5(b). In the absence of PH, propagating chains retain the Br chain ends. In the presence of PH, the nucleophilic substitution reaction of a propagating chain with PH terminates the chain and produces an aromatic end-group. Together, these results show that PH increases dispersity via chain termination due to a nucleophilic substitution reaction, and suggest that PH concentration can be used as a design parameter to systematically tune dispersity of polymers synthesized via conventional ATRP.

Table 3. ¹H NMR peak area ratios for the ATRP of tBA with various amounts of PH^a

[PH]:[EBiB]	Peak area ratio for protons on initiator fragment and end group: c:(b+g)	Peak area ratio for protons on polymer repeat units: (f+d):e	Peak area ratio for protons in <i>meta</i> and <i>para</i> position on PH end group: x:(b+g)	Nucleophilic substitution product yield ^b
0:1	2.03	11.05	0	0
1:1	2.52	11.08	0.48	38%
3:1	2.56	11.07	0.67	53%

^a Theoretical ratios in the absence of chain termination: c:(b+g) = 2 and (f+d):e = 11.

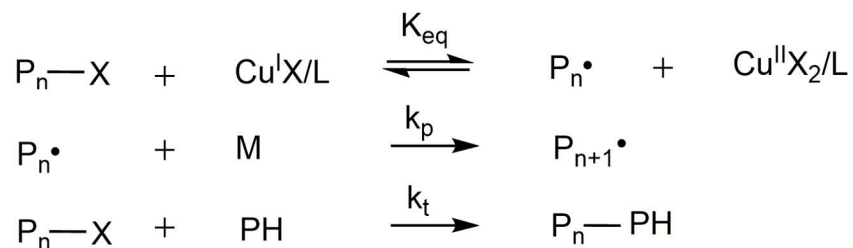
^b Side product yield: $100 \cdot (2A_x)/(A_c)$, where A_x and A_c are the respective areas of peaks x and c

We developed a kinetic model to describe ATRP reactions in the presence of a chain terminating agent (here, PH). In addition to the conventional ATRP reaction steps, we also incorporated chain termination due to nucleophilic substitution (Scheme 2). First, we assumed that the ATRP reactions undergo fast initiation and rapid approach equilibrium, conditions necessary to achieve low \bar{D} in the absence of PH.⁵⁸ Second, we neglected chain termination outside of the reaction with PH. Finally, we assumed that [PH] was much higher at any given time point than the dormant chain concentration [PX] due to fast ATRP equilibrium. After solving the rate equations (detailed in the ESI), we obtained a rate equation of the form

$$\ln \left(\frac{[M]_0}{[M]} \right) = \frac{A}{B} (1 - e^{-Bt}); \quad A = \frac{k_p K_{eq} [Cu(I)][PX]_0}{[Cu(II)]}, \quad B = k_{PH}[PH] \quad (3)$$

Although the values of the parameters in A and B are not known, we may nonetheless fit kinetic data for reactions conducted in the presence of PH to the functional form in eqn 3. We obtained excellent agreement between the model (eqn 3) and the experimental kinetic data obtained in

reactions with [PH]:[EBiB]= 1:1 and 3:1 (Figure 6), further confirming our proposed reaction mechanism in Figure 5(b) and validating the assumptions used in deriving the model. We anticipate that this approach and the derived equation will be valid for any ATRP synthesis with the addition of a chain terminating agent reacting with the alkyl halide following the same stoichiometry as described in Scheme 2.



Scheme 2. ATRP equilibrium, propagation, and termination (with PH) reactions.

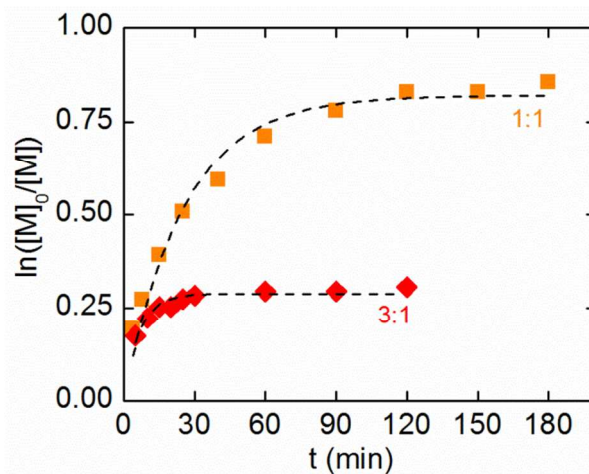


Figure 6. Kinetic data ($\ln([M]_0/[M])$ as a function of reaction time) for the ATRP of tBA conducted in the presence of PH. Dashed curves show the model fit (eqn 3) to experimental data obtained from ATRP syntheses conducted with [PH]:[EBiB] = 1:1 (orange ■) and 3:1 (red ◆). Excellent agreement between the model and data confirms the presence of chain termination with addition of PH in ATRP. Parameters A and B were 0.03 and 0.04, respectively, for [PH]:[EBiB] = 1:1, and 0.04 and 0.15, respectively, for [PH]:[EBiB] = 3:1.

Addition of PH to Modify Dispersity in the ATRP of Styrene

To test the broad applicability of PH addition for modulating dispersity in ATRP syntheses, we employed polystyrene as a second model system. ATRP of styrene was conducted under varying ratios of [PH]:[EBiB] (0:1, 0.2:1, 1:1, 3:1), keeping the concentrations of the other reagents identical to those used in the synthesis of PtBA. For each reaction, aliquots were taken at regular intervals to determine $M_{n,GPC}$ and \mathcal{D} under varying ratios of [PH]:[EBiB] (Table S2 in the ESI). The dispersity of polystyrene was tuned over a broad range through addition of PH (Figure 7). \mathcal{D} ranged from 1.07 to 2.30, depending on the reaction time and on [PH]:[EBiB] (Figure 7(a)), and increasing [PH]:[EBiB] led to greater $M_{n,GPC}$ for a given conversion (Figure 7(b)). High ratios of [PH]:[EBiB] (1:1 and 3:1) produced polymers with high dispersities, but the reaction conversion was low and did not change significantly upon increasing the reaction time. When the lower ratio [PH]:[EBiB] = 0.2:1 was employed, the reaction conversion increased with reaction time and polymers with dispersities of $\mathcal{D} = 1.14 - 1.53$ were obtained. This proof-of-concept experiment demonstrated that varying the reaction time and ratio of [PH]:[EBiB] generated polymers with controllable \mathcal{D} in the range of 1.1 – 2.3.

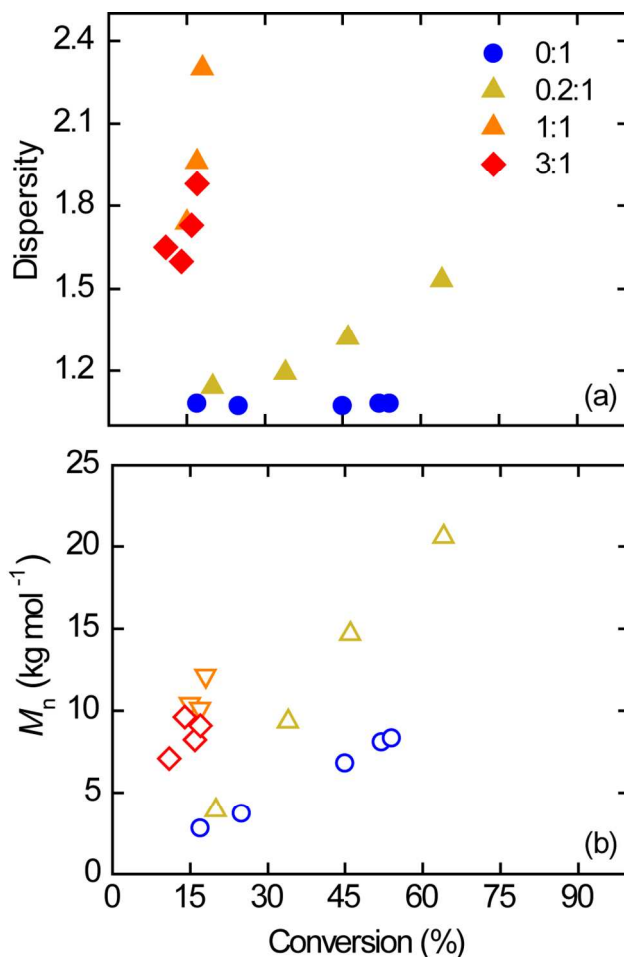


Figure 7. Dispersity (a) and $M_{n,GPC}$ (b) as functions of monomer conversion for the ATRP of styrene in the presence of different ratios of [PH]:[EBiB]: 0:1 (blue ●), 0.2:1 (mustard ▲), 1:1 (orange ▼), and 3:1 (red ◆). Closed symbols signify dispersity and open symbols signify M_n . A broad range of dispersities ($1.07 < \mathcal{D} < 2.30$) for PS can be obtained by adding PH. M_n and \mathcal{D} were measured with GPC using light scattering (triple detection). The following reaction conditions were employed: [EBiB]:[CuBr]:[PMDETA]:[styrene] = 1:1:1:120, 80 °C, toluene.

Conclusions

We investigated the effect of phenyl hydrazine (PH) addition on the synthesis of poly(*tert*-butyl acrylate) (PtBA) using ATRP. The presence of PH markedly increased the dispersity of the synthesized polymer. Reactions conducted with PH showed deviations from the expected kinetic behavior for ATRP syntheses: 1) the monomer conversion achieved a plateau at low to moderate conversion and subsequently did not change with increased reaction time, 2) the reaction kinetics were inconsistent with existing models (Matyjaszewski and Fischer's

equations), and 3) the initial reaction rate was higher than a comparable reaction conducted without PH addition.

To test the hypothesis that the increase in dispersity arises from the action of PH as a reducing agent in the ATRP synthesis, we examined the effect of another common ATRP reducing agent, tin(II) 2-ethylhexanoate. Surprisingly, addition of tin(II) 2-ethylhexanoate did not increase the polymer dispersity. Next, we examined the possibility of chain termination in reactions conducted in the presence of PH. Polymerizations conducted with PH showed a lack of end-group fidelity through characterization of the relative concentration of initiator fragments and Br end-groups, consistent with the presence of chain termination. By contrast, polymerizations without PH addition exhibited the expected relative concentrations of initiator fragments and Br end-groups. The presence of aromatic end-groups in reactions conducted in the presence of PH confirmed the chain termination mechanism due to nucleophilic substitution. We developed a kinetic model that accounted for chain termination, which showed excellent agreement with experimental data. Finally, we showed that addition of PH could be used to tune the dispersity of polystyrene, indicating that this method is not limited to PtBA but can be applied to other polymer systems. In summary, PH is an effective modifier for ATRP syntheses, providing systematic control over the dispersity of polymers containing unimodal molecular weight distributions. A method to tailor dispersity has broad potential practical applications, as variation in dispersity can enhance compatibility of polymer blends, modulate the response of polymers grafted to a surface, alter the morphology of block copolymers, and improve polymer processability.

Electronic Supplemental Information (ESI). The following are included in the Electronic Supplementary Information (ESI): Reaction scheme of *tert*-butyl acrylate polymerization (Scheme S1); ^1H NMR spectrum for fully purified and dried PtBA synthesized without PH addition ($[\text{PH}] : [\text{EBiB}] = 0:1$) (Figure S1); ^1H NMR spectra for PtBA synthesized without phenylhydrazine addition ($[\text{PH}]:[\text{EBiB}] = 0:1$) at different reaction times (Figure S2); GPC refractometer data for PtBA synthesized without PH ($[\text{PH}]:[\text{EBiB}] = 0:1$) at different reaction times (Figure S3); ^1H NMR spectrum for fully purified and dried PtBA synthesized with PH addition ($[\text{PH}] : [\text{EBiB}] = 1:1$) (Figure S4); ^1H NMR spectra for PtBA synthesized with phenylhydrazine addition ($[\text{PH}]:[\text{EBiB}] = 1:1$) at different reaction times (Figure S5); GPC refractometer data for PtBA synthesized with PH ($[\text{PH}]:[\text{EBiB}] = 1:1$) at different reaction times (Figure S6); ^1H NMR spectrum for fully purified and dried PtBA synthesized with PH addition ($[\text{PH}] : [\text{EBiB}] = 3:1$) (Figure S7); ^1H NMR spectra for PtBA synthesized with phenylhydrazine addition ($[\text{PH}]:[\text{EBiB}] = 3:1$) at different reaction times (Figure S8); GPC refractometer data for PtBA synthesized with PH ($[\text{PH}]:[\text{EBiB}] = 3:1$) at different reaction times (Figure S9); Characterization of PtBA synthesized using various ratios of $[\text{PH}]:[\text{EBiB}]$ at different reaction times (Table S1); ^1H NMR spectra for PtBA synthesized in the presence of tin (II) 2-ethylhexanoate (Figure S10); Characterization of PS synthesized using various ratios of $[\text{PH}]:[\text{EBiB}]$ at different reaction times (Table S2); Detailed calculation for end-group analysis in presence of PH and derivation of model; MALDI-TOF data and analysis (Figures S11-S14 and Table S3).

Acknowledgements. We are grateful to Christopher Pennington for assistance with MALDI sample preparation, data collection, and analysis. We thank Ramanan Krishnamoorti and Richard Willson for insightful discussions. MLR gratefully acknowledges support from the National

Science Foundation under Grant No. CBET-143783. JCC acknowledges funding from the National Science Foundation (DMR-1151133) and the Welch Foundation (E-1869).

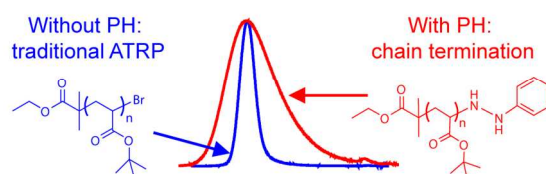
References

1. D. G. Hassell, J. Embery, T. C. B. McLeish and M. R. Mackley, *Journal of Non-Newtonian Fluid Mechanics*, 2009, **157**, 1-14.
2. A. Allal, A. Lavernhe, B. Vergnes and G. Marin, *Journal of Non-Newtonian Fluid Mechanics*, 2006, **134**, 127-135.
3. M. Ansari, Y. W. Inn, A. M. Sukhadia, P. J. DesLauriers and S. G. Hatzikiriakos, *Journal of Rheology*, 2013, **57**, 927-948.
4. D. Roy, C. B. Giller, T. E. Hogan and C. M. Roland, *Polymer*, 2015, **81**, 111-118.
5. X. Ye and T. Sridhar, *Macromolecules*, 2005, **38**, 3442-3449.
6. J. K. Nielsen, H. K. Rasmussen, O. Hassager and G. H. McKinley, *Journal of Rheology*, 2006, **50**, 453-476.
7. S. G. Hatzikiriakos, *Polymer Engineering & Science*, 2000, **40**, 2279-2287.
8. L. Di Landro, M. Levi, D. Nichetti and A. Consolo, *European Polymer Journal*, 2003, **39**, 1831-1838.
9. M. Nadgorny, D. T. Gentekos, Z. Xiao, S. P. Singleton, B. P. Fors and L. A. Connal, *Macromolecular Rapid Communications*, 2017, **38**, 1700352-n/a.
10. L. Li, Y. Huang and Q. Yang, *Journal of Macromolecular Science, Part B*, 2011, **50**, 2140-2149.
11. D. Broseta, G. H. Fredrickson, E. Helfand and L. Leibler, *Macromolecules*, 1990, **23**, 132-139.
12. C.-T. Lo, S. Seifert, P. Thiyagarajan and B. Narasimhan, *Macromol. Rapid Commun.*, 2005, **26**, 533-536.
13. N. A. Lynd and M. A. Hillmyer, *Macromolecules*, 2005, **38**, 8803-8810.
14. N. A. Lynd and M. A. Hillmyer, *Macromolecules*, 2007, **40**, 8050-8055.
15. A. L. Schmitt and M. K. Mahanthappa, *Soft Matter*, 2012, **8**, 2294-2303.
16. J. M. Widin, A. K. Schmitt, K. Im, A. L. Schmitt and M. K. Mahanthappa, *Macromolecules*, 2010, **43**, 7913-7915.
17. J. M. Widin, A. K. Schmitt, A. L. Schmitt, K. Im and M. K. Mahanthappa, *J. Am. Chem. Soc.*, 2012, **134**, 3834-3844.
18. N. A. Lynd, A. J. Meuler and M. A. Hillmyer, *Progress in Polymer Science*, 2008, **33**, 875-893.
19. D. T. Gentekos, J. Jia, E. S. Tirado, K. P. Barteau, D.-M. Smilgies, R. A. DiStasio and B. P. Fors, *Journal of the American Chemical Society*, 2018, **140**, 4639-4648.
20. V. Kottisch, D. T. Gentekos and B. P. Fors, *ACS Macro Letters*, 2016, **5**, 796-800.
21. W. M. de Vos and F. A. M. Leermakers, *Polymer*, 2009, **50**, 305-316.
22. V. Yadav, Y. Jaimes-Lizcano, N. Dewangan, N. Park, T.-H. Li, M. Robertson and J. Conrad, *ACS Applied Materials & Interfaces*, 2017, **9**, 44900-44910.
23. V. Yadav, A. V. Harkin, M. L. Robertson and J. C. Conrad, *Soft Matter*, 2016, **12**, 3589-3599.
24. T. B. Martin and A. Jayaraman, *Soft Matter*, 2013, **9**, 6876-6889.
25. M. Rubinstein and R. H. Colby, *The Journal of Chemical Physics*, 1988, **89**, 5291-5306.
26. D. C. Venerus, E. F. Brown and W. R. Burghardt, *Macromolecules*, 1998, **31**, 9206-9212.
27. S. Trinkle and C. Friedrich, *Rheologica Acta*, 2001, **40**, 322-328.
28. F. J. Stadler, C. Piel, J. Kaschta, S. Rulhoff, W. Kaminsky and H. Münstedt, *Rheologica Acta*, 2006, **45**, 755-764.
29. G. J. P. Britovsek, S. A. Cohen, V. C. Gibson, P. J. Maddox and M. van Meurs, *Angewandte Chemie-International Edition*, 2002, **41**, 489-491.
30. G. J. P. Britovsek, S. A. Cohen, V. C. Gibson and M. van Meurs, *Journal of the American Chemical Society*, 2004, **126**, 10701-10712.

31. W. H. Carothers, *Transactions of the Faraday Society*, 1936, **32**, 39-49.
32. J.-S. Wang and K. Matyjaszewski, *Macromolecules*, 1995, **28**, 7901-7910.
33. G. Moad, E. Rizzardo and S. H. Thang, *Australian Journal of Chemistry*, 2005, **58**, 379-410.
34. C. J. Hawker, A. W. Bosman and E. Harth, *Chemical Reviews*, 2001, **101**, 3661-3688.
35. D. T. Gentekos, L. N. Dupuis and B. P. Fors, *Journal of the American Chemical Society*, 2016, **138**, 1848-1851.
36. R. B. Grubbs, *Polymer Reviews*, 2011, **51**, 104-137.
37. N. Corrigan, A. Almasri, W. Taillades, J. Xu and C. Boyer, *Macromolecules*, 2017, **50**, 8438-8448.
38. K. Matyjaszewski, *Macromolecules*, 2012, **45**, 4015-4039.
39. R. Barbey, L. Lavanant, D. Paripovic, N. Schüwer, C. Sugnaux, S. Tugulu and H.-A. Klok, *Chemical Reviews*, 2009, **109**, 5437-5527.
40. S. Karanam, H. Goossens, B. Klumperman and P. Lemstra, *Macromolecules*, 2003, **36**, 3051-3060.
41. G. Kickelbick and K. Matyjaszewski, *Macromol. Rapid Commun.*, 1999, **20**, 341-346.
42. L. Delaude, S. Delfosse, A. Richel, A. Demonceau and A. F. Noels, *Chemical Communications*, 2003, DOI: 10.1039/B301733H, 1526-1527.
43. J. Xia, S. G. Gaynor and K. Matyjaszewski, *Macromolecules*, 1998, **31**, 5958-5959.
44. P. Kwiatkowski, J. Jurczak, J. Pietrasik, W. Jakubowski, L. Mueller and K. Matyjaszewski, *Macromolecules*, 2008, **41**, 1067-1069.
45. K. Pan, L. Jiang, J. Zhang and Y. Dan, *Journal of Applied Polymer Science*, 2007, **105**, 521-526.
46. J. Huang, T. Pintauer and K. Matyjaszewski, *Journal of Polymer Science Part A: Polymer Chemistry*, 2004, **42**, 3285-3292.
47. K. Matyjaszewski, W. Jakubowski, K. Min, W. Tang, J. Huang, W. A. Braunecker and N. V. Tsarevsky, *Proceedings of the National Academy of Sciences*, 2006, **103**, 15309-15314.
48. G. Y. Li, S. Song, L. Guo and S. M. Ma, *J. Polym. Sci. Pol. Chem.*, 2008, **46**, 5028-5035.
49. E. Berndt, S. Behnke, A. Dannehl, A. Gajda, J. Wingender and M. Ulbricht, *Polymer*, 2010, **51**, 5910-5920.
50. Q. Liu and Y. Chen, *Journal of Polymer Science Part A: Polymer Chemistry*, 2006, **44**, 6103-6113.
51. O. Bertrand, J.-M. Schumers, C. Kuppan, J. Marchand-Brynaert, C.-A. Fustin and J.-F. Gohy, *Soft Matter*, 2011, **7**, 6891-6896.
52. M. Suchoparek and J. Spevacek, *Macromolecules*, 1993, **26**, 102-106.
53. K. Ibrahim, B. Löfgren and J. Seppälä, *European Polymer Journal*, 2003, **39**, 2005-2010.
54. W. Lin, Q. Fu, Y. Zhang and J. Huang, *Macromolecules*, 2008, **41**, 4127-4135.
55. Q. Fu, W. Lin and J. Huang, *Macromolecules*, 2008, **41**, 2381-2387.
56. H. Fischer, *Journal of Polymer Science Part A: Polymer Chemistry*, 1999, **37**, 1885-1901.
57. H. Zhang, B. Klumperman, W. Ming, H. Fischer and R. van der Linde, *Macromolecules*, 2001, **34**, 6169-6173.
58. K. Matyjaszewski, T. E. Patten and J. Xia, *J. Am. Chem. Soc.*, 1997, **119**, 674-680.
59. A. Snijder, B. Klumperman and R. van der Linde, *Macromolecules*, 2002, **35**, 4785-4790.
60. P. Kryszewski and K. Matyjaszewski, *European Polymer Journal*, 2017, **89**, 482-523.
61. S. P. Zhu, *Macromol. Theory Simul.*, 1999, **8**, 29-37.
62. S.-i. Yamamoto and K. Matyjaszewski, *Polym. J.*, 2008, **40**, 496-497.
63. Y. Kwak and K. Matyjaszewski, *Polymer International*, 2009, **58**, 242-247.
64. S. R. Woodruff, B. J. Davis and N. V. Tsarevsky, in *Progress in Controlled Radical Polymerization: Mechanisms and Techniques*, American Chemical Society, 2012, vol. 1100, ch. 7, pp. 99-113.

TOC Graphic

Tuning Dispersity in ATRP with Phenylhydrazine (PH) Addition



Phenyl hydrazine is an effective modifier for ATRP syntheses, providing systematic control over the dispersity of polymers with unimodal molecular weight distributions.